euronoise

Spectral properties of the surface SH waves in a vertically periodic half-space

Stanislav Golkin, Olivier Poncelet and Alexander Shuvalov

LMP, UMR CNRS 5469, Université Bordeaux I, 351, cours de la Libération, 33405 Talence, France
o.poncelet@lmp.u-bordeaux1.fr

The paper is concerned with propagation of shear horizontal (SH) surface waves in semi-infinite media with vertically periodical continuous or discrete variation of material properties. Generally, the dispersion branches of these waves come about as broken intervals within random spectral ranges where the 'physical' solution exists. The more striking it is that the spectrum of SH surface wave may often have a perfectly regular spectral structure. The present study is focused on one of the most interesting cases, which is when the surface wave exists within only a single velocity window and does not exist elsewhere or vice versa. This occurs in particular if the material variation over unit cell is monotonic. Inverting the trend of monotonicity swaps two aforementioned types of spectra. Assuming simple examples of a linearly inhomogeneous and bilayered unit cells, we first calculate the surface-wave dispersion spectrum in the (ω, k) domain and then obtain the same spectrum by post-signal processing of the FDTD (Finite Difference Time Domain) simulated wave field. A good agreement between the two spectra validates theoretical predictions.

1 Introduction

Surface acoustic waves acquire some striking particularities when the material properties have a periodical dependence along the vertical axis directed into the depth of the medium. In such a case, the surface-wave dispersion branches may extend down to zero horizontal slowness and they may come about in the form of randomly broken intervals.

Further specificity characterizes the spectra of SH (shear horizontal) surface waves propagating in a vertically periodic half-space with a vertical symmetry plane. It is that the branches of 'physical' and 'non-physical' SH surface waves, attributed as such due to their decrease or increase into the depth, are the alternating intervals of the dispersion curves of actually another spectrum, namely, the spectrum for guided waves in a single unit cell (period) considered as a free layer. This feature has been noted for periodic stacks of homogeneous layers [1-5] generalized for an arbitrary continuous or piecewise continuous vertically periodic media [6]. The problem of finding SH surface waves reduces therefore to calculating the dispersion branches of a free unit-cell layer and to identifying their spectral ranges which render the wave 'physical'.

Generally speaking, the SH surface wave may be expected to exist on some unordered 'fragments' of the reference unit-cell spectrum and these can be determined only through a numerical procedure of testing the radiation condition. Interestingly though, the spectral ranges of surface-wave existence can often be predicted without any calculations, by merely inspecting certain basic benchmarks of a given profile of variation of material constants over unit cell. For a broad class of inhomogeneity profiles, the dispersion spectrum of SH surface wave appears to be perfectly regular in that it is confined in between certain velocity bounds.

A direct link between the profile shape and the surface-wave existence is especially compelling when the material properties are monotonic over a period. For instance, if the velocity and impedance of the shear bulk waves are both decreasing over a period then the range of existence of SH surface wave on the dispersion curves is 'squeezed' to a narrow velocity window, which actually admits a simple and explicit evaluation. For an inverse, increasing profile the surface wave does not exist in this window and exists elsewhere. An analytical proof relies on the properties of the ordinary differential equation with periodically varying coefficients which governs the SH wave propagation in the (ω, k) space. Such spectral selectivity may be interesting for applications. The objective of the present paper is to simulate the aforementioned phenomenon in the space-time domain and to compare the results with the prediction obtained in the transform domain.

2 Background of the problem in the (ω, k) space

2.1 Equation of motion

Given is a unidirectionally inhomogeneous medium with the density $\rho = \rho(y)$ and stiffness tensor $c_{ijkl} = c_{ijkl}(y)$ varying along axis Y. The tensor c_{ijkl} is supposed to have a symmetry plane XY. Consider the SH wave propagating in this plane and polarized orthogonally to it. The wave displacement is sought in the form

$$u(\mathbf{r},t) = A(y)e^{i\varphi}, \varphi = \exp\left\{\mathrm{i}\omega\left[s\left(x - \int_0^y \frac{c_{45}}{c_{55}}\mathrm{d}\varsigma\right) - t\right]\right\}, \quad (1)$$

where ω is the frequency and s is the slowness along the axis X. The equation of motion may be written in the form

$$\mathbf{Q}(y)\boldsymbol{\eta}(y) = \boldsymbol{\eta}'(y) \quad (2)$$

with

$$\mathbf{Q}(y) = \mathrm{i}\omega\begin{pmatrix} 0 & 1/c_{44} \\ \rho - C_{55}s^2 & 0 \end{pmatrix}, \boldsymbol{\eta}(y) = \begin{pmatrix} \mathrm{i}\omega A(y) \\ c_{44}A'(y) \end{pmatrix} \quad (3)$$

and $C_{55} = c_{55} - c_{45}^2 / c_{44}$. The solution to (2), related to an initial condition $\boldsymbol{\eta}(y_0)$ at any y_0, is

$$\boldsymbol{\eta}(y) = \mathbf{M}(y, y_0)\boldsymbol{\eta}(y_0), \quad (4)$$

where $\mathbf{M}(y, y_0)$ is the 2x2 matricant or propagator. It expands into Peano series of multiple integrals [7-9]

$$\mathbf{M}(y, y_0) = \begin{pmatrix} M_1(y, y_0) & M_2(y, y_0) \\ M_3(y, y_0) & M_4(y, y_0) \end{pmatrix} = \\ = \mathbf{I} + \int_{y_0}^{y} \mathbf{Q}(y_1)\mathrm{d}y_1 + \int_{y_0}^{y}\int_{y_0}^{y_1} \mathbf{Q}(y_1)\mathbf{Q}(y_2)\mathrm{d}y_1\mathrm{d}y_2..., \quad (5)$$

where $\mathbf{I}$ is identity matrix.

2.2 Periodicity

We now specify the inhomogeneity along Y as periodic, so that $\mathbf{Q}(y) = \mathbf{Q}(y + T)$ where T denotes the least period. Each unit cell $y \in [0, T]$ may be a stack of different

homogeneous or inhomogeneous layers in welded contact maintaining continuity of $\boldsymbol{\eta}(y)$, or it may be a single continuously inhomogeneous layer. Two SH Floquet modes [9] are associated with the eigenspectrum of the propagator $\mathbf{M}(T,0)$ through the period

$$\mathbf{M}(T,0)\mathbf{w}_\alpha = q_\alpha \mathbf{w}_\alpha \ (\alpha = 1,2),\ q_1 = 1/q_2 \equiv e^{\mathrm{i}KT}, \quad (6)$$

where K is the Floquet wavenumber. Obviously,

$$\mathbf{M}(NT,0)\mathbf{w}_\alpha = q_\alpha^N \mathbf{w}_\alpha \ (\alpha = 1,2). \quad (7)$$

For a given T, the propagator $\mathbf{M}(T,0)$ and hence its eigenvectors $\mathbf{w}_\alpha$ and eigenvalues q_α depend on ω and $s = k/\omega$. The plane $\{\omega, k\}$ is therefore mapped out into the passbands, where q_1 and q_2 are complex conjugated numbers of a unit absolute value (K is real), and the stopbands, where q_1 and q_2 are real (K is purely imaginary). The lines $q_1 = q_2 (= \pm 1)$ are the stopband edges.

2.3 Dispersion equation

The SH surface wave in a vertically periodic halfspace must satisfy the condition $\sigma_{23} \sim A' = 0$ on the traction-free surface $y = 0$ and also the radiation condition, which demands decrease of surface-wave amplitude into the depth. For the latter reason, the appropriate ('physical') wave solutions lie strictly inside the stopbands and correspond there to that one of two SH Floquet modes $\alpha = 1,2$, for which the (real) eigenvalue of $\mathbf{M}(T,0)$ is such that $|q_\alpha| < 1$. This inequality does imply that SH surface wave consists of a single Floquet mode but, on this grounds solely, it may yet be either the mode $\alpha = 1$ or the mode $\alpha = 2$. Now we recall the traction-free boundary condition $A'(0) = 0$. A single Floquet mode fulfils the latter condition at $y = 0$, and simultaneously at all interfaces $y = NT$ (see (7)), if and only if it corresponds to the eigenvector $\mathbf{w}_\alpha$ of $\mathbf{M}(T,0)$ with an identically vanishing second (related to A') component. The required form $\mathbf{w}_\alpha \parallel (1,0)$ demands that $M_3(T,0) = 0$ and, given so, it selects a single Floquet mode exceptionally as the mode $\alpha = 1$, for which $M_3(T,0) = 0$ implies $q_1 = M_1(T,0)$. Thus, by (4) with $y_0 = 0$ and $\boldsymbol{\eta}(0) = A(0)\mathbf{w}_\alpha$, the wave amplitude at $y = NT$ after any number N of periods is $A(NT) = M_1^N(T,0)A(0)$. It remains now to come back to the aforementioned radiation condition $|q_\alpha| < 1$ and to fix $\alpha = 1$ in there, thus asking that

$$|A(T)| = |M_1(T,0)A(0)| < |A(0)|. \quad (8)$$

Recapping the above arguments, the dispersion spectrum for SH surface wave in a semi-infinite periodic structure is defined by a pair of conditions

$$\begin{cases} M_3(T,0) = 0, \\ |M_1(T,0)| \left(= |M_4(T,0)|^{-1}\right) < 1, \end{cases} \quad (9)$$

with the entries given by (5). Finding the spectrum, say in the form of frequency versus wavenumber dependence $\omega(k)$, amounts to a two-step procedure. The first step is solving Eq. $(9)_1$ from which we calculate the dispersion branches for SH guided waves in a free inhomogeneous layer $y \in [0,T]$ consisting of one period of a given structure (see [10] for more details). The second step is applying the inequality $(9)_2$ to identify the spectral intervals on these branches where the SH surface wave exists.

3 Surface-wave spectral corridor: prediction and verification

3.1 Continuously inhomogeneous unit cell

We consider a periodically inhomogeneous isotropic half-space with a traction-free surface $y = 0$ and a monotonically decreasing profile over unit cell. To illuminate the principal features in question, we confine to a simple example of a linear velocity profile

$$c_t(y) = c_t(0)\left(1 - \frac{y - nT}{4T}\right), \quad (10)$$

where $c_t(y) = \sqrt{c_{44}/\rho}$, n is the number of the unit cell, T is the least period, and

$$c_t(0) = 1\ mm/\mu s,\ T = 1\ mm. \quad (11)$$

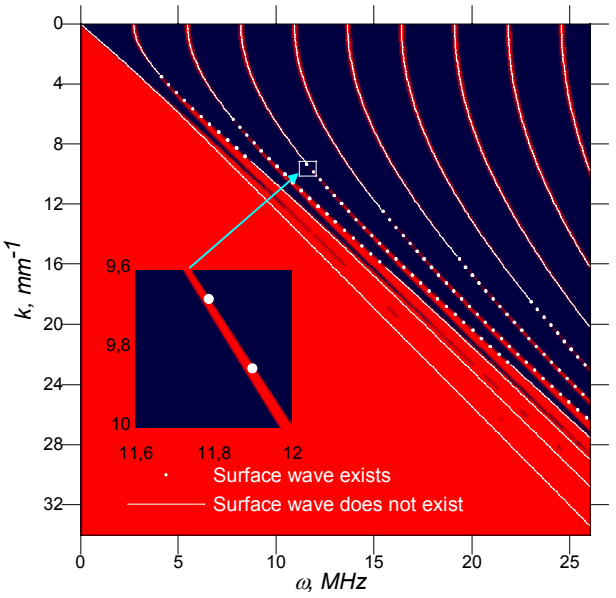

Fig. 1. Dispersion curves calculated in the (ω, k) space and overlayed onto the Floquet passbands (black zones) and stopbands (red zones, which appear as grey in black and white display). The stopbands near cutoffs are narrow and therefore not well resolved to the scale of the plot (see a zoomed inset).

The density $\rho = 1\,g/cm^3$ is assumed constant. The dispersion branches calculated in the transform domain (ω, k) from Eqs. (5) and (9) are shown in Fig. 1. These branches lie inside the Floquet stopbands and include 'physical' parts, where the amplitude decreases into the depth and hence the surface wave exists, and the non-physical part, where the amplitude increases and the surface wave does not exist. The velocity window (spectral corridor on the $\{\omega, k\}$ plane) of the surface-wave existence lies within asymptotically constant lower and upper velocity bounds $c_1 \lessapprox \omega/k \lessapprox c_2$, which can be estimated by a simple and general formula involving only the values of $\rho(y)$ and $c_t(y)$ at the unit-cell edges $y = 0, T$. For the assumed case of a constant density, this formula simplifies to

$$c_1 \lessapprox \max\left\{c_t(0), c_t(T)\right\},\ c_2 \approx \sqrt{c_t^2(0) + c_t^2(T)}. \quad (12)$$

Inverting the monotonicity profile swaps the surface-wave existence and non-existence zones.

We shall now verify the aforementioned predictions by simulating a time-space SH wave field in a periodic half-space by means of the second-order FDTD (Finite Difference Time Domain) method.

The numerical procedure is as follows. A surface punctual source generating SH transient signal is taken in the form

$$F(\mathrm{r},t) = \delta(\mathrm{r}-\mathrm{r}_0)\frac{\sin(8\pi(t-t_0))}{8\pi(t-t_0)}\mathrm{e}^{-0.05(t-t_0)^2}, \qquad (13)$$

where r_0 is a point on the surface. This source is applied to the stress component σ_{23} only. This type of signal is advantageous, because its frequency spectrum is almost a rectangular window

$$0 \le f = \omega/2\pi \le 4\,MHz \qquad (14)$$

with a constant amplitude for any frequency within the window. Therefore it enables getting numerical dispersion diagrams of approximately the same order of magnitude in the range $[0,4\,MHz]$ just by one simulation. The FDTD scheme is implemented for 20 inhomogeneous periodic unit cells with the profile (10). We choose $\Delta x = \Delta y = 0.025\,mm$ as dimensions for the cells in the numerical code, and a computational domain of $(40\,mm, 30\,mm)$ which corresponds to a grid of 1600×1200 cells along X and Y, respectively. At the highest frequency in the simulation ($f_{\max} = 4\,MHz$) the least wavelength in the domain ($\lambda_{\min} = 0.1875\,mm$) is sampled by 7.5 points. The time step is $\Delta t = 0.0075\,\mu s$ and the simulation runs over 16384 steps (approximately $123\,\mu s$). The PMLs (Perfectly Matched Layers) are added at the bottom and both edges for modeling a semi-infinite half-space. The computational domain and the duration of the simulation are large enough for the surface wave to form itself in space and time. Thereby, taking signals $S(t_i), i = 1..n$ at m points on the surface we create a table $S(t_i, x_j), i = 1..n, j = 1..m$. Then 2D FFT (Fast Fourier Transform) is applied to this table in order to visualize dispersion curves in the (ω,k) domain as spectrum intensity images. In order to increase the resolution of those images (i.e. decreasing Δk and $\Delta\omega$) we have performed zero-padding over spatial and temporal data. It also allows us not to probe signals at each point along the surface but to pick signals periodically (basically one point over four along the surface was probed for the images presented in this paper). For example, the resolution in Figs. 2 and 3 are $\Delta k \approx 0.08\,mm^{-1}$ (which is four times smaller than the Δk stemming from the raw data) and $\Delta\omega \approx 0.05\,MHz$. Due to such a procedure, the images are neater and trajectories of dispersion curves are much more discernible.

Fig.2 compares the dispersion curves calculated directly in the (ω,k) domain (see Fig. 1) with those obtained by means of post-signal processing of the FDTD-simulated wave field. A good correspondence between both spectra is observed.

Let us see what happens for an increasing linear profile, which is inverse to (10), i.e., defined by

$$c_t(y) = c_t(0)\left(1-\frac{nT-y}{4T}\right). \qquad (15)$$

According to the analytical derivation in the (ω,k) space, the surface wave should now exist where it did not exist for the decreasing profile (10) and vice versa. Fig. 3 demonstrates good agreement of this prediction with the FDTD numerical results.

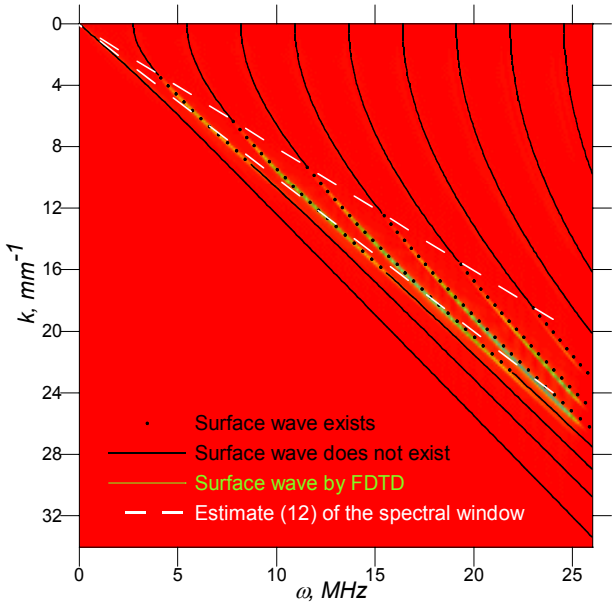

Fig. 2. Superposition of the dispersion curves calculated in the (ω,k) domain with the curves obtained by FDTD. The profile of unit-cell inhomogeneity is given by (10)

Note that a slight shift in Fig. 3 between the curves, calculated in the (ω,k) domain and obtained by FDTD is due to the numerical dispersion of FDTD scheme. Eliminating this drawback is important for high-frequency implementation. This is possible by way of taking more points per wave length; on the other hand, doing so entails growth of the computational domain. Thus getting better precision of the numerical results at high frequency requires increasing computational time and RAM memory capacity.

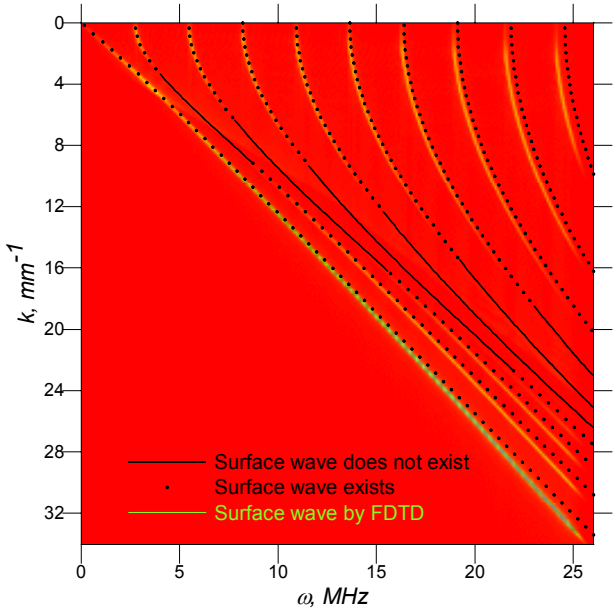

Fig. 3. The same as in Fig. 2 for the increasing profile (15) inverse with respect to (10)

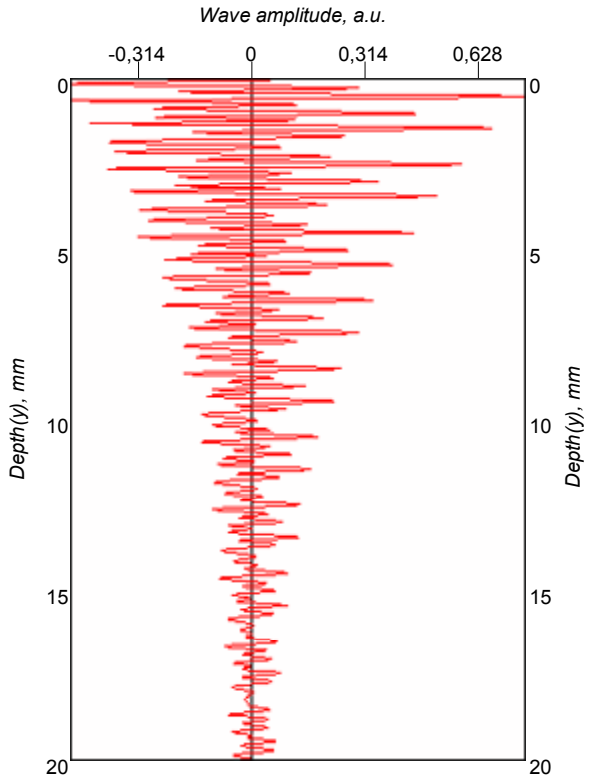

Fig. 4. Dependence of the FDTD-simulated SH wave field on the vertical coordinate y for the profile (15), taken for $t = 123\,\mu s$ at a distance $13.75\,mm$ from the source.

For confirming consistency of our surface-wave modeling, we also calculate the distribution of signal amplitude through the depth at a fixed time, which is taken long enough to attain a stable wave amplitude profile. This occurs after the principal wave front emitted by the source reaches the edges of the computational domain and disappears within PMLs. As soon as it no longer affects the wave field, we observe the wave field produced by reflections and transmissions at the interfaces between unit cells. Fig. 4 shows an exponential decrease into the depth, which confirms the surface-wave type localization as predicted by the theory.

3.2 Piecewise homogeneous unit cell

We now briefly consider a periodically bilayered isotropic half-space. Both layers constituting the unit cell have constant values of density and velocity, which are taken as follows

$$\rho_1 = \rho_2 = 1\,g/cm^3, c_{t1} = 2\,mm/\mu s, c_{t2} = 1\,mm/\mu s, \quad (16)$$

where the subscript 1 and 2 indicate the upper and lower layers. Obviously, any bilayered unit cell has a discretely monotonic profile. In the case (16) the velocity (and impedance) decreases into the depth of the unit cell. Hence the SH surface wave must exist in a narrow velocity window. Its bounds are given by the same equation (12) as in the case of a continuously inhomogeneous unit cell, except that the lower bound and its evaluation become exact. Thus $c_1 \le \omega/k \lessapprox c_2$, where

$$c_1 \lessapprox \max\left\{c_{t1}, c_{t2}\right\},\ c_2 \approx \sqrt{c_{t1}^2 + c_{t2}^2}\,. \quad (17)$$

For the simulation, we take a surface punctual source in the same form as in (13), but with the factor 8π replaced by 2π in order to decrease the calculation time, which is affordable for a relatively simple case in hand. The frequency spectrum of generated signal has a form of almost rectangular window

$$0 \le f = \omega/2\pi \le 1\,MHz\,. \quad (18)$$

The FDTD scheme is implemented for 20 bilayered unit cells. We chose $\Delta x = \Delta y = 0.1\,mm$ and $\Delta t = 0.017\,\mu s$. Computational domain is $(260\,mm, 40\,mm)$ that is 2600x400 grid. Implementing the same procedure as described in § **3.1,** we obtain the curves which are displayed in Fig. 5 alongside the results of the direct calculation in the (ω, k) space. It is noted that (16) assumes the velocity contrast over unit cell such that is stronger higher than it was taken above in (10) (2:1 and 1:0.75, respectively), so the surface-wave velocity window in the present case is broader. This is confirmed by Fig. 5 but may elude the first glance due to a different frequency scale relatively to Fig. 2.

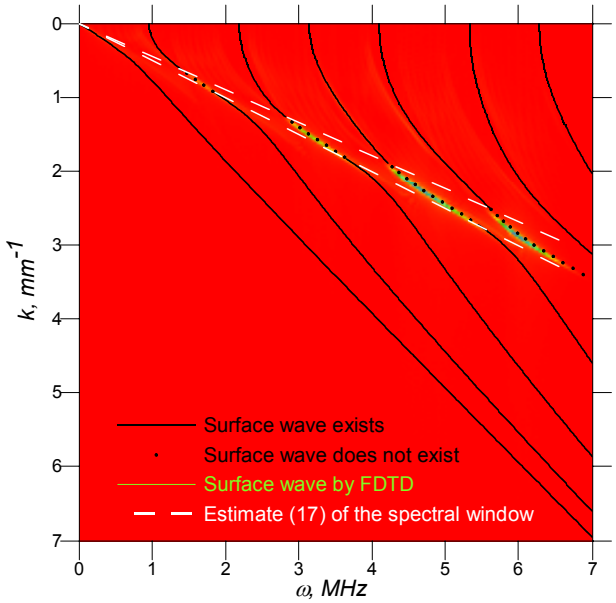

Fig. 5. Superposition of the dispersion curves calculated in the (ω, k) domain with the curves obtained by FDTD for the bilayered unit cell defined in (16)

The results for the inverse case of discretely increasing unit cell with

$$\rho_1 = \rho_2 = 1\,g/cm^3,\ c_{t1} = 1\,mm/\mu s, c_{t2} = 2\,mm/\mu s \quad (19)$$

are presented in Fig. 6. As expected, the spectral zones of surface-wave existence and non-existence swap with respect to Fig. 5.

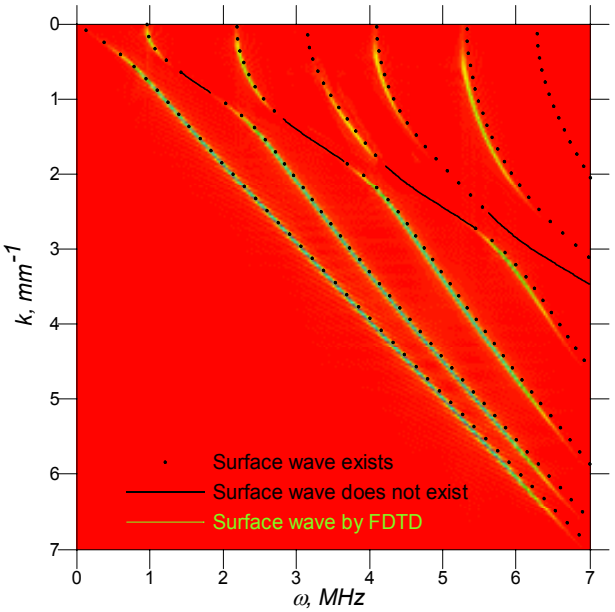

Fig. 6. The same as in Fig. 5 for the inverted profile, given by (19)

4 Conclusion

A particular spectral selectivity phenomenon has been demonstrated for the SH surface wave in a vertically periodic half-space with a monotonic profile of material properties variation over period. For this case, the theory predicts that the surface wave exists within only a single velocity window and does not exist elsewhere or vice versa, the alternative depending on whether the profile is decreasing or increasing. Simple examples of a linearly inhomogeneous and a bilayered unit cell were considered. The surface-wave dispersion spectra have been obtained in two dufferent ways: computed in the (ω, k) space and extracted from FDTD-simulated wave field. The spectra visualize the expected spectral window or gap, containing or precluding the surface-wave branches. A good agreement between both calculations validates consistency of modeling.

References

[1] R. E. Camley, B. Djafari-Rouhani, L. Dobrzynski and A. A. Maradudin, "Transverse Elastic Waves in Periodically Layered Infinite and Semi-infinite Media", Phys. Rev. B **27**, 7318-7329 (1983).

[2] E. H. El Boudouti, B. Djafari-Rouhani, A. Akjouji and L. Dobrzynski, "Theory of Surface and Interface Elastic Waves in N-layer Superlattices", Phys. Rev. B **54** 14728-14741 (1996).

[3] P. Gatignol, C. Potel and J. F. d. Belleval, "Two families of modal waves for periodic structures with two field function: a Cayleigh-Hamilton approach", Acustica-Acta Acustica **96**, 959-975 (2007).

[4] A. N. Podlipenets, "Surface Love Wave in Orthotropic Regularly Layered Composites", Mech. Comp. Matter. **18**, 734-737 (1982).

[5] N. A. Shul'ga, "Propagation of Elastic Waves in Periodically Inhomogeneous Media", Int. Appl. Mech. **39**, 763-796 (2003).

[6] A. L. Shuvalov, O. Poncelet and A. N. Podlipenets, "On the guided and surface shear horizontal waves in monoclinic transversely periodic layers and halfspace with arbitrary variation of material peroperties across the unit cell", Stud. Geophys. Geod. **50**, 381-398 (2006).

[7] K. Aki and P. G. Richards, *Quantitative seismology* (Freeman and C , San Francisco, 1980).

[8] B. L. N. Kennett, *Seismic Wave Propagation in Stratified Media* (Cambridge, 1983).

[9] M. C. Pease III, *Method of Matrix Algebra* (Academic Press, New York, 1965).

[10] A. L. Shuvalov, O. Poncelet and A.P. Kiselev, "Shear horizontal waves in transversely inhomogeneous plates", Wave Motion **45**, 605-615 (2008).